LA-UR-97- 2954

Approved for public release; distribution is unlimited.

TITLE: TEXTURE AND RESIDUAL STRAIN IN SIC/TI-6-2-4-2 TITANIUM MATRIX COMPOSITES

CONF-970691--

AUTHOR(S): Partha Rangaswamy, LANSCE 12
Kristin Bennett, LANSCE 12
Mark A. M. Bourke, LANSCE 12
N. Jayaraman, University of Cincinnati
Robert Von Dreele, LANSCE 12
Joyce A. Roberts, LANSCE 12

SUBMITTED TO: The V International Conference on Residual Stresses (ICRS-V)
Linkoping University
Linkoping Sweden
June 16 -18, 1997

Los Alamos
NATIONAL LABORATORY

Form No. 836 R5
ST 2629 10/91

DISCLAIMER

Texture and residual strain in SiC / Ti-6-2-4-2 Titanium Matrix Composites

[1]Partha Rangaswamy*, [1]Kristin Bennett, [1]Mark A. M. Bourke, [2]N. Jayaraman, [1]Robert Von dreele, [1]Joyce A. Roberts,
[1]Manuel Lujan Jr. Neutron Scattering Center, H 805
Los Alamos National Laboratory
Los Alamos, New Mexico 87545
USA

[2]Department of Materials Science and Engineering
University of Cincinnati
Cincinnati, Ohio 45221-0012
USA

* Email: partha@lanl.gov
http://www.lansce.lanl.gov/mlnsc

Abstract:

Residual strain and texture variations were measured in two Titanium matrix composites reinforced with Silicon Carbide fibers (Ti/SiC) having the same composition but fabricated by dramatically different processing routes. In both specimens the Titanium matrix comprised an α/β alloy (Ti-6242) containing approximately 35% by volume of continuous SiC fibers. In one case the matrix was produced by a plasma spray (PS) route and the other by a wire drawing (WD) process. The resulting textures in the matrix differ significantly, from approximately random for the PS matrix to 6.25X random in the WD matrix. No significant differences in matrix residual strains between the composites prepared by the two procedures were noted. Plane-specific elastic moduli, measured in load tests on the unreinforced matrices also showed little difference.

1. Introduction:

Titanium Matrix Composites (TMCs) continuously reinforced with silicon carbide (SiC) fibers have received considerable attention in the past, due to their potential to replace conventional titanium and nickel-base alloys in aerospace systems such as advanced turbine engines and hypersonic vehicles [1-3], where specific strength and stiffness at high temperatures are critical. However one concerns in the development of TMCs is the presence of residual stresses and their influence on fracture stress, toughness, fatigue resistance and other mechanical properties of these composites. Due to the inherent two-fold mismatch in the coefficient of thermal expansion between the titanium matrix and of the SiC reinforcement and fabrication temperatures around 900°C, residual stresses develop. For some TMCs, calculations estimate the matrix residual stresses to be as high as 75% of the yield strength of the matrix material [4]. These stresses are expected to be high enough to cause localized matrix-yielding around the fiber matrix interface in ductile materials or even cracking in some brittle matrices.

Despite extensive characterization of TMCs in the past measurement and modeling of residual stresses faces a growing challenge because of the new processes that result in more complicated or highly textured microstructures. Owing to the anisotropic nature of the hexagonal lattice, preferred orientation of the α phase plays an important role in determining the mechanical behavior in titanium alloys with a significant volume fraction of this phase [*]. Since residual stresses develop during consolidation of the Titanium composites, the role of residual stresses in the mechanical behavior of titanium composites has been well studied [4-7]. One of the new processes is

for **some** TMCs is wire drawing, which involves winding both the matrix in the form of wire and the fibers together on a large drum, using a small amount of binder followed by HIPing (see figure 1). The composite samples in the form of panels are then age-heat-treated. This type of process results in a strongly textured material. Models used for predicting residual stresses and their effects on lifetime predictions have to be validated. Therefore, it is important for residual stresses to be experimentally determined in these textured materials. In aircraft engine components texture or mechanical anisotropy must be accounted in order to achieve reliable design parameters. Conversely, if the anisotropy is known, it should be possible to exploit it in the design and life analysis of the part. As a result, significant economic benefits are predicted for the use of these alloys in selected engine components.

The objective of this study is to demonstrate characterization of texture and strain two TMCs using a pulse neutron diffraction source technique. These results are compared with a similar TMC's processed with a plasma spray process, which results in the titanium matrix having a random texture [6,18]. The comparison exposes the effects (or absense thereof) of processing route.

2. Approach:

Diffraction techniques (x-ray & neutron) are viable techniques for the measurements of strain or texture in TMCs because of the polycrystalline nature of the constituents. However X-ray stress measurements are restricted to surface and matrix only [8-18] and may in some circumstances not be representative of the interior [13]. Alternatively, neutron strain measurement can measure residual strains in both the constituents [**].

The majority of measurements to date are reported for systems that have random or mild texture, because "strong" texture in the matrix material of the composite tends to hinder measurement by X-rays on indeed monochromatic neutron sources. In the Xrd case for "strongly" textured materials such tilting methods may not work because the diffraction peak dissappears as the sample is tilted. Even in neutron diffraction techniques when the source of the neutrons is from a reactor (monochromatic beam of neutrons) similar restrictions may exist although it is less of a problem since tilting is not a prerequisite.

However, when a pulse source is used, due to the polychromatic nature of the incident neutron beam, many different lattice reflections are possible and assuming there the texture allows it a reflection can always be found in any geometry. Neutron Powder Diffractometer (NPD) at Los Alamos National Laboratory that is used for measuring residual strains has this inherent advantage of the pulse source [13,18]. This leads to using multiple peaks to calculate the strains (residual & applied), and from this information a distinction between isotropic and anisotropic behavior of the reflections and the individual constinuents can be discerned.

3. Specimen Preparation:

The wire drawn (WD) composites were produced by Atlantic Research Corporation (ARC) using Ti-6Al-2Sn-4Zr-2MO wire and Trimarc-1(SiC) fibers. The 178 μm Ti-6242 cold drawn wire was bought from a commercial weld-wire source according to AMS specification 4975-F. The 127 μm SiC fibers were bought from Americom and were produced by their joint venture with 3M. The fiber was produced by the CVD deposition of SiC onto a tungsten monofilament and the subsequent deposition of ~ 3μm of carbon in a 3-layered outer coating. The circular mat was slit across the drum, yielding a large, rectangular mat. Panels were cut to the appropriate size, bagged, outgassed to remove the binder, and then HIP'd and then aged. Specimens were cut to a size of 100 mm x 25 mm from these panels by water jet cutting, then diamond ground. The composite samples were 10 ply, with a nominal volume fraction of fibers being 35%. From X-ray studies we determined that the matrix Ti-6242 was 95% alpha (HCP) and 5% beta (BCC). There the residual strain analysis was limited to alpha phase only and the strain in the beta phases was assumed to be negligible.

The plasm sprayed (PS) TMCs were fabricated at Textron Specialty Materials [7]. In the plasma spray process, superheated droplets of Ti-6242 matrix is deposited on silicon carbide fibers (SCS-6) wound on a rotating and axially translated drum surface. Some of the advantages of the plasma spray process are fiber swimming is virtually eliminated because the fiber is rigidly held in place by the sprayed metal. No added ribbon or wire is required and because the process uses powder, almost any matrix can be selected. The 136 μm SiC fibers (SCS-6) were bought from Textron Specialty Materials, Inc. The fiber was produced by the CVD deposition of SiC onto a carbon monofilament and the subsequent deposition of ~ 6μm of carbon in a 3-layered outer coating. The plasma sprayed fiber monotape and foil are cut into appropriate panel sizes. These are subsequently stacked for fabrication of the TMC using a hot-isostatic-press (HIP). Metallography of the the plasma sprayed matrix of the composite revealed an equiaxed $\alpha + \beta$ microstructure. Similar to the textured matrix, the matrix had about 90 % alpha (HCP) and 10% beta (BCC) as measured using X-ray diffraction techniques. The fiber volume fraction (v_f) was 31%. Specimens measuring 12 x 100 x 1.25 mm were cut from the panels.

4. Texture Measurements on High Intensity Powder Diffractometer (HIPD) :

Samples of the matrix alone and composites measuring 20 mm x 50 mm were placed in the neutron beam. Polychromatic neutron radiation and a High Intensity Neutron Diffractometer (HIPD) were used to determine texture in two samples of the neat matrix material and the composite [**]. Each sample was mounted on a two-circle goniometer with the fiber direction perpendicular to the incident neutron beam. The sample was rotated in the plane perpendicular to the incident beam (about the pole figure angle χ) and with respect to the Bragg angle of diffraction (2θ). The changes in the relative intensity of the diffraction peaks with respect to the angular rotations were recorded. In addition, using the six detector banks on HIPD, six different diffraction vectors were measured at each orientation setting. Diffraction patterns taken at a sufficient number of sample orientations were then fitted with a Rietveld refinement procedure, using a spherical harmonics description of the texture in Generalized Structural Analysis System (GSAS) to determine complete pole figures [19,20]. **Figure 2(a,b)** show the pole figures for the WD and PS matrices of the composites for the prism plane (10.0), basal plane (00.1) and the pyramid plane (11.1) respectively. The pole figure for the textured matrix represents a strong fiber texture with the normal to the prism planes (10.0) oriented in the rolling direction. Transverse to the rolling direction, a strong texture of the (00.1) planes was observed. The texture analysis shows that the matrix of the texture composite could be considered as a pseudo-single crystal oriented with the basal pole "(00.2) pole" aligned transverse to the rolling direction. Note that in some orientations a small proportion of the grains did not possess the ideal texture.

5. Residual Strain Measurements on Neutron Powder Diffractometer (NPD) :

Neutron diffraction is performed "routinely" on the Neutron Powder Diffractometer at LANL [**]. In the use of a Neutron Spallation Source for strain measurement, strains are measured out of all the grains (having different hkls) within the sampling volume. These are bulk measurements, and the strains are an average over many grains. Strains from different hkls are measured simultaneously, making this technique extremely useful and unique for studying this class of systems. The main limiting factor of strain measurements using textured and texture-free samples is the availability of all the reflections on texture-free samples, compared to working with only few reflections in textured samples.

Strain direction is defined by the scattering vector. Thus, with the fibers oriented at 45° to the beam, the four banks provide simultaneous strain measurements at 0°, 29°, 61° and 90° to the fiber direction [18]. Measurements were made in two orientations: First, the detectors at ±90 degrees measured the longitudinal $\langle\varepsilon_{LL}\rangle_{Long}$ and through thickness $\langle\varepsilon_{NN}\rangle_{Long}$ strains. In the second, the transverse $\langle\varepsilon_{TT}\rangle_{Trans}$ and $\langle\varepsilon_{NN}\rangle_{Trans}$ through thickness strains were recorded. This procedure was

adopted as a check to verify if the strains measured were the principal strain components. The irradiated volume was ~ 840 mm^3 and count periods of ~ 6 hours at a beam current of 70μA were used.

Bragg reflections were fitted individually and strains (ε_{hkl}) were calculated by comparison of the composite with samples of monolithic alloy or fibers according to;

$$\varepsilon_{hkl} = (d_{hkl} - d_o)/d_o \quad (1)$$

where d_{hkl} and d_o are the interplanar spacings in the composite and unstressed standard, respectively, and hkl are the Miller indices of the diffracting planes. As mentioned previously, the main limiting factor between strain measurements using textured and untextured samples is the availability of all the reflections on untextured samples, compared to working with only few reflections in textured samples as shown in **figure (3a,b).** Only the reflections which offered the best resolution in terms of peak fits were used for strain calculations. A total of twelve hk.l reflections (10.0, 00.2, 10.1, 11.0, 20.0, 10.3, 11.2, 20.1, 00.4, 21.1, 11.4, 30.0) in the matrix and five hk.l reflections (11.0, 22.0, 31.1, 42.2, 33.1, 51.1) in the fibers were used to calculate the strain in the matrix and the fiber. Strong texture variations were observed between the composites and monolithics.

6. Results and Discussion:

The objective of this study was to demonstrate the use of neutron powder diffractometer spallation technique for measurement of strains in textured TMCs, and to compare the strains with measurements made on a similar but untextured TMCs.

Plane-Specific-Elastic-Strains (PSES) in the individual components (matrix and fiber) of the composite material were measured by taking the differences in the d-spacings of the diffracting planes (hk.l) from the constituents of the TMCs and a representative strain-free standard. Residual strains in both the matrix and the fiber were determined with the specimens oriented in the longitudinal and transverse orientations as shown in **figure 4**. Consistent with expectations the residual strain in the matrix is tensile and that in the fiber is compressive both in the transverse and longitudinal orientations.

In figure 4a (longitudinal orientation) generally the strains decrease in both the matrix and fiber with increasing α going from 0 to 90°. Due to strong fiber texture in the matrix, only prism planes (10.0, 20.0, 30.0) produced diffraction peaks at $\alpha = 0°$. For $\alpha = 29$, 57 and 90°, basal (00.2,00.4), prism (11.0) and pyramidal planes (10.1,11.2) planes produced diffraction peaks. Variation in the strains for the three (10.0), (20.0) and (30.0) prism planes is within ± 5 % of the average elastic strain of approximately 3500 με. For $\alpha = 90°$ the measured strains for different hk.ls ranges from + 48 to + 2219 (με), with the prism plane (11.0) showing the lowest value and the basal planes (00.2) showing the highest value. Once again we see that the two basal (00.2), (00.4) planes used for measurement of the strains are within ± 5 %. In contrast to the results from longitudinal fiber orientation (Figure 4a), the results for transverse orientation (Figure 4b) showed no specific preference of the diffracting planes for various angles of β. This is to be expected since the material was shown to have a fiber texture with the fiber axis parallel to the longitudinal fiber orientation. Similar to the trend observed in the longitudinal fiber orientation (Figure 4a) the residual strains which is indicative of a transversely isotropic system. This is further confirmed by the that in the transverse orientation residual strains measured from one set of diffracting planes do not show significant variation with changing angle of β (figure 4b) from 0 to 90°. Additionally, these values are also similar to the strains measured for the corresponding planes in the longitudinal orientation (figure 4a) at $\alpha = 90°$. In the longitudinal orientation, figure 4a, for those diffracting planes which produce diffraction peaks at two or more angles of α (10.1,11.0, and 20.1) there is a trend of decreasing residual strains with increasing α angle is observed. In the case of residual strains in the fibers similar trends are observed for the longitudinal and transverse orientations, excepting all of these strains are of compressive in nature.

Figures 5a and 5b are plots of measured strain for the orientations shown in the longitudinal and transverse directions for the untextured TMC. Unlike the the textured TMCs all crystallographic planes produce diffractions at all orientations. But, similar to the textured material the untextured material in the longitudinal orientation showed highest strain values for $\alpha = 0$ and lowest strain values for $\alpha = 90$ for any set of crystallographic planes. Similarly in the transverse orientation the untextured material showed very little variation in strains with varying β angles.

Figure 6 shows a direct comparison of the plane-specific strains for the textured and untextured matrix. If the strain magnitudes are the same for the respective hk.l between the textured and random-textured matrix material, they should essentially fall on the straight line. Within experimental errors intrinsic within the measurement process and the fact that the reinforcements (SiC fibers) used are not identical, except stochiometrically, these results surprisingly show that there seem to be no significant difference in the hk.l strain distribution between the textured and untextured matrix materials.

Another significant difference between the textured and the untextured TMCs is the strain values measured in the fibers. The untextured TMC showed significantly lower values of compressive strains both in the longitudinal and transverse orientation in comparison with the strains observed in the textured TMCs. It is presumed that these difference in the fiber strains could be attributed to the differences in the fiber manufacturing process and differences in the phases present in the fibers. In order to fully understand these observations a complete analysis of the three dimensional stress and strain state of both TMCs have to be conducted.

Plane-specific elastic constants were determined using the in-situ loading measurements of the monolithic materials on neutron powder diffractometer. These values are tabulated for both texture and un-textured monolithic matrix materials in **Table I**. These values are also compared with calculations of plane specific elastic constants made using stiffness constants S_{11}, S_{12}, S_{13}, S_{33}, S_{44} for pure single crystal Titanium. There was a reasonable comparison between experimental and predicted values.

The plane-specific residual stresses (σ_{hkls}) were in turn determined by using the measured strains from Figure 4 and 5 and the corresponding elastic constants from **Table I**. These values are listed in **Table II**. From the results shown in **Table III**, it appears that the plane-specific residual stresses are comparable between the textured and untextured material. This is so in spite of the fact that the textured material lends few diffraction planes for this analysis.

Based on these stresses and measured strains a more detailed stress/strain analysis is underway to account for all the observations

7. Summary and Conclusions:

Texture and residual strain variations were measured in two TMCs having the same composition but fabricated by a wired drawn (textured) and plasma spray (untextured) processes respectively. Texture and residual strains and stresses for the matrix of the composites are compared. The following is a summary of the results and observations based on our study.

- Texture measurements on the Wire Drawn matrix revealed a significant fiber texture measuring 6.25X random with the fiber axis pointing in [10.0] direction of the HCP unit cell and transversely isotropic. In comparison, the Plasma Spray matrix exhibited random texture.
- Comparison of the plane specific matrix residual strains (tensile) between the textured and untextured TMC showed no significant differences, despite in the untextured TMC diffraction was observed from all planes in all orientations while in the textured TMC diffraction was limited

to specific planes depending on the orientation. In both cases the longitudinal orientations showed a continuos decrease in strain values with increasing angle from the fiber direction to the normal to the fiber direction. However in the transverse orientation no significant differences were observed at various angles.

- The trend seen with regard to residual strains (compressive) in the fiber in both TMCs were similar but the textured TMC showed significantly higher level of residual strains in comparison with the untextured TMC. This difference is attributed to the possible differences in phase contents of the reinforcing fibers in the two TMCs.

Based on the above results we can conclude that, in spite of the fact that the textured TMCs lends few diffraction planes for measurement of, the neutron spallation technique can be used successfully. In addition the presence of texture appeared to have little effect on plane specific strains. A more detailed stress/strain analysis to fully understand the implications of these observations is in progress.

8. Acknowledgements:

The Manuel Lujan Jr. Neutron Scattering Center is a national user facility funded by the United States Department of Energy, Office of Basic Energy Science and Defense Programs. This work was supported in part by DOE contract ~~W-7405-ENG-36~~. We acknowledge Jim Larsen, Kathy Stevens of WL/MLLN for providing the textured samples and permission to disseminate this information and for useful discussions in preparation of this manuscript.

9. References:

1. J.M. Larsen, K.A. Williams, S.J. Balsone, and M.A. Stucke: 1990, High Temperature Aluminides and Intermetallics. S.H. Whang, C.T. Liu, D.P. Pope, J.O. Stiegles, Eds., TMS/ASM International, USA, pp. 521-556.
2. J.M. Larsen, W.C. Revelos, and M.L. Gambone: 1992, Intermetallic Composites II., D.B. Miracle, D.L. Anton, and J.A. Graves, Eds., MRS Proceedings, Vol. 273, 1992 Pittsburgh, PA. Reference in press:
3. N. Ashbaugh, M. Khobaib, R. John, et al: "Mechanical Properties of Advanced Engine Materials", Final Report, Air Force Contract WL-TR-91-4149; Wright-Patterson Air Force Base, OH (April 1992).
4. P.K. Wright, "Thermal Stress Effects in Intermetallic Matrix Composites", Residual Stresses in Composites: Measurement, Modeling and Effect on Thermo-Mechanical Properties, Ed. E.V. Barrera, I. Dutta, and S.G. Fishman, TMS, 1993.
5. W.S. Johnson, S.J. Lubowinski, and A.L. Highsmith: Thermal and Mechanical Behavior of Ceramic and Metal Matrix Composites, ASTM STP 1080, J.M. Kennedy, H.H. Moeller, and W.S. Johnson, Eds. Philadelphia, 1990, pp. 193-218.
6. H. Gigernzer, and P. K. Wright: " Plasma Sprayed SCS-6/Titanium Aluminide Composite Test Panels", Titanium Aluminide Composites, P.R. Smith, S.J. Balsone, and T. Nicolas, Eds., WL-TR-91-4020, pp. 251-264.
7. C.A. Bigelow, W.S. Johnson and A.R. Naik: "A comparison of various micromechanics models for metal matrix composites", Mechanics of Composite Materials and Structures. Eds: J.N. Reddy and J.L. Telpy, 1989.
8. M.R. James, "Residual Stresses in Metal Matrix Composites", International Conference on Residual Stresses II. eds. G. Beck, S. Denis and A. Simon, Elsevier, pp. 429-35 (1989).
9. P. Rangaswamy, W.C. Revelos and N. Jayaraman: "Residual stresses in SCS-6/Ti-24Al-11Nb Composite: Part 1- Experimental"; Journal of Composites and Technology Research, (JCTRER), Vol. 16, No. 1, January 1994, pp. 47-53.
10. P. Rangaswamy, and N. Jayaraman, "Residual stresses in SCS-6/Beta-21S Metal Matrix Composites", Journal of Composites and Technology Research, (JCTRER), Vol. 17, No. 1, January 1995, pp. 43-49.
11. B.N. Cox, M.R. James, D.B. Marshall, and R.C. Addison, Jr:"Determination of Residual Stresses in Thin Sheet Titanium Aluminide Composites", Metallurgical Transactions A, 1990, Vol. 21 A, pp 2701.
12. M.R. James, "Behavior of Residual Stresses during Fatigue of Metal Matrix Composites", Residual Stresses-3, ed. H. Fujiwara, T. Abe and K. Tanaka, Elsevier, pp 555-560 (1992).
13. M.R. James, M.A. Bourke, J.A. Goldstone and A.C. Lawson: "Residual Stress Measurements in Continuous Fiber Titanium Matrix Composites", Advances in X-ray Analysis, Vol. 36., (1993).

14. Paul S. Prevey, "A method of determining the elastic properties of alloys in selected crystallographic directions for X-ray diffraction residual stress measurement", Advances in X-ray Analysis, Vol 20, Pg 345-354.
15. A. Saigal, D.S. Kupperman and S. Majumdar: "Residual Strains in Titanium Matrix, High Temperature Composites", Materials Science and Engineering, 1992, AI50, pp. 59-66.
16. S. Majumdar, J.P. Singh, D. Kupperman and A.D. Krawitz, Application of Neutron Diffraction to Measure Residual Strains in Various Engineering Composite Materials, J. Eng. Mat. and Tech., 113:51-59 (1991).
17. D.S. Kupperman, S. Majumdar, J.P. Singh, "Residual Strain in Adavanced Composites", Neutron News, 2:15-18 (1991).
18. P. Rangaswamy, M.A.M. Bourke, P.K. Wright, E. Kartzmark, J. Roberts & N. Jayaraman, "Influence of residual stresses on the Thermo-mechanical processing of SCS-6/Ti-6-2-4-2 Titanium Metal Matrix Composites ", accepted for publication in Materials Science & Engineering (1996).
19. R.B. Vondreele, J.D. Jorgensen and C.G. Windsor, "Rietveld Refinement with Spallation Neutron Powder Diffraction Data", J. Applied Crystal 15: 581-589. (1982).
20. A.C. Larson and R. B. Vondreele. "GSAS - Generalized Structural Analysis System.", Report: LAUR 86-748. Los Alamos National Laboratory. (1994).

Table 1

Comparison of Plane Specific Elastic Constants from experimental measurements and from analytical predictions

HKLs	E_{hkl} - **Texture** (Wire-drawn) **(GPa)**	E_{hkl} - **Untexture** (Plasma - Sprayed) **(GPa)**	E_{hkl} - **Single Crystal predictions*** **(GPa)**
100	**110**	**111**	**103**
002	**148**	**140**	**145**
101	**116**	**111**	**108**
110		**112**	**104**
112		**97**	**109**
201	**110**	**108**	**104**

*Note: This are based on the five independent stiffness constants S_{11}, S_{12}, S_{13}, S_{33},S_{44}

Table 2

Neutron Calculated Stresses for Textured and Un-Textured matrix material

(//) Parallel to fiber - Matrix Stresses

Plane Specific Elastic Constants **(PSEC)**	σ_{hkl} - **Texture** (Wire-drawn) **(MPa)**	σ_{hkl} - **Untexture** (Plasma-Sprayed) **(MPa)**
100,200,300	**379**	**362**
002,004		**596**
101		**419**
110		**444**
112		**365**
201	**404**	**460**

(⊥) Perpendicular to fiber - Matrix Stresses

Plane Specific Elastic Constants **(PSEC)**	σ_{hkl} - Texture (Wire-drawn) **(MPa)**	σ_{hkl} - Untexture (Plasma-Sprayed) **(MPa)**
100,200,300		
002,004	**315**	**312**
101	**112**	**94**
110		**70**
112		**41**
201		**105**

Note: The σ_{hkls} represented are calculated simply by multiplying the measured PSECs (from Table 2) by the appropriate elastic strains measured from figure 4a for α=0°, 90°.

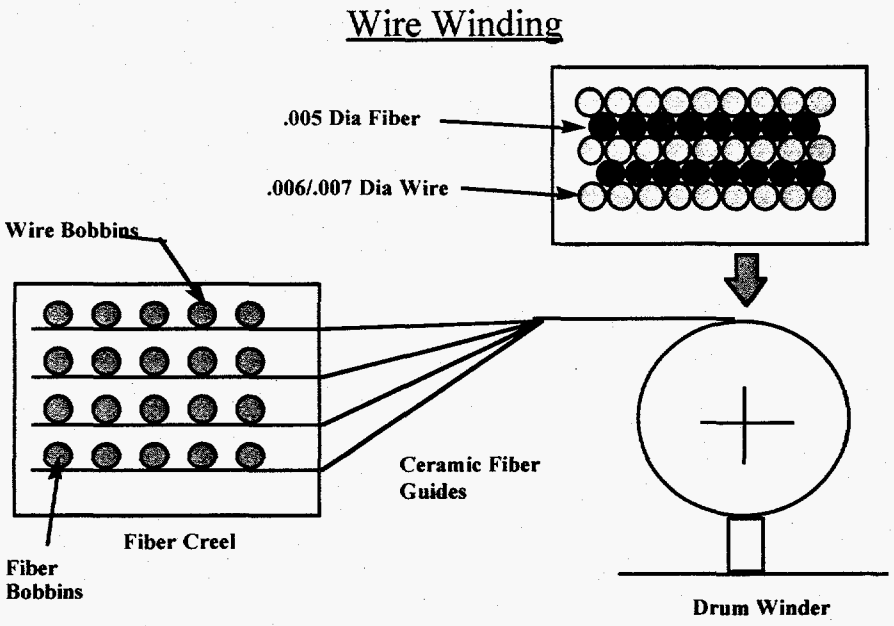

(a)

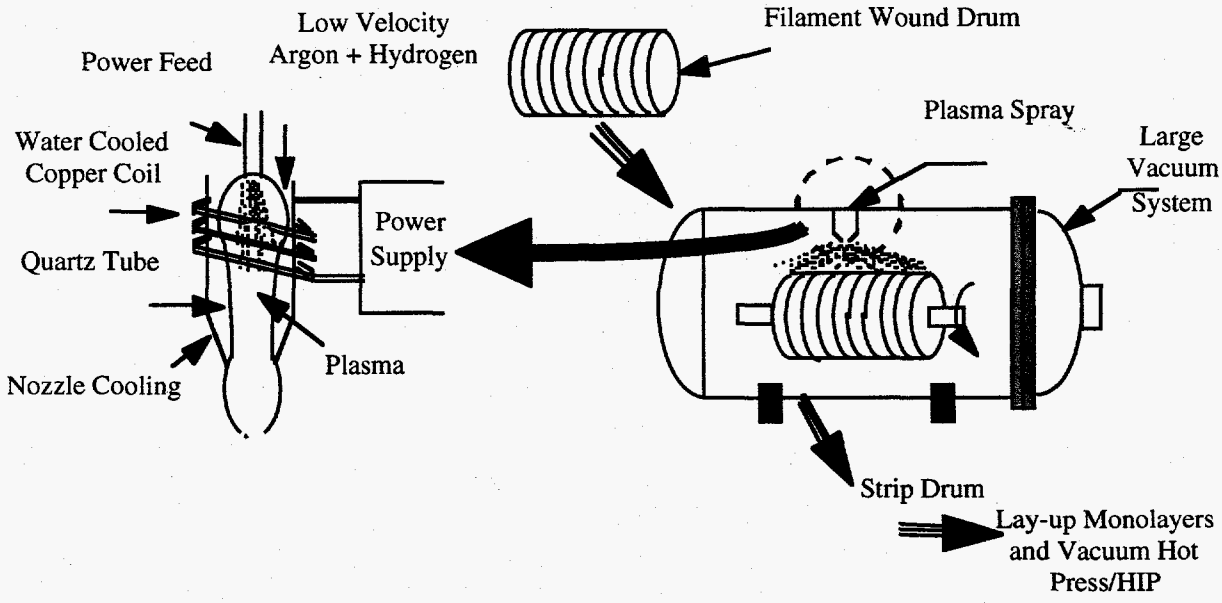

(b)

Figure 1. Schematic of the (a) Wire Winding technique and (b) RF Induction Plasma Deposition (Plasma Spray) technique used in fabricating the SiC/Ti Metal Matrix Composites.

Bulk Texture Pole figures of Titanium Matrix in Composite Plasma Sprayed Vs. Wire Drawn

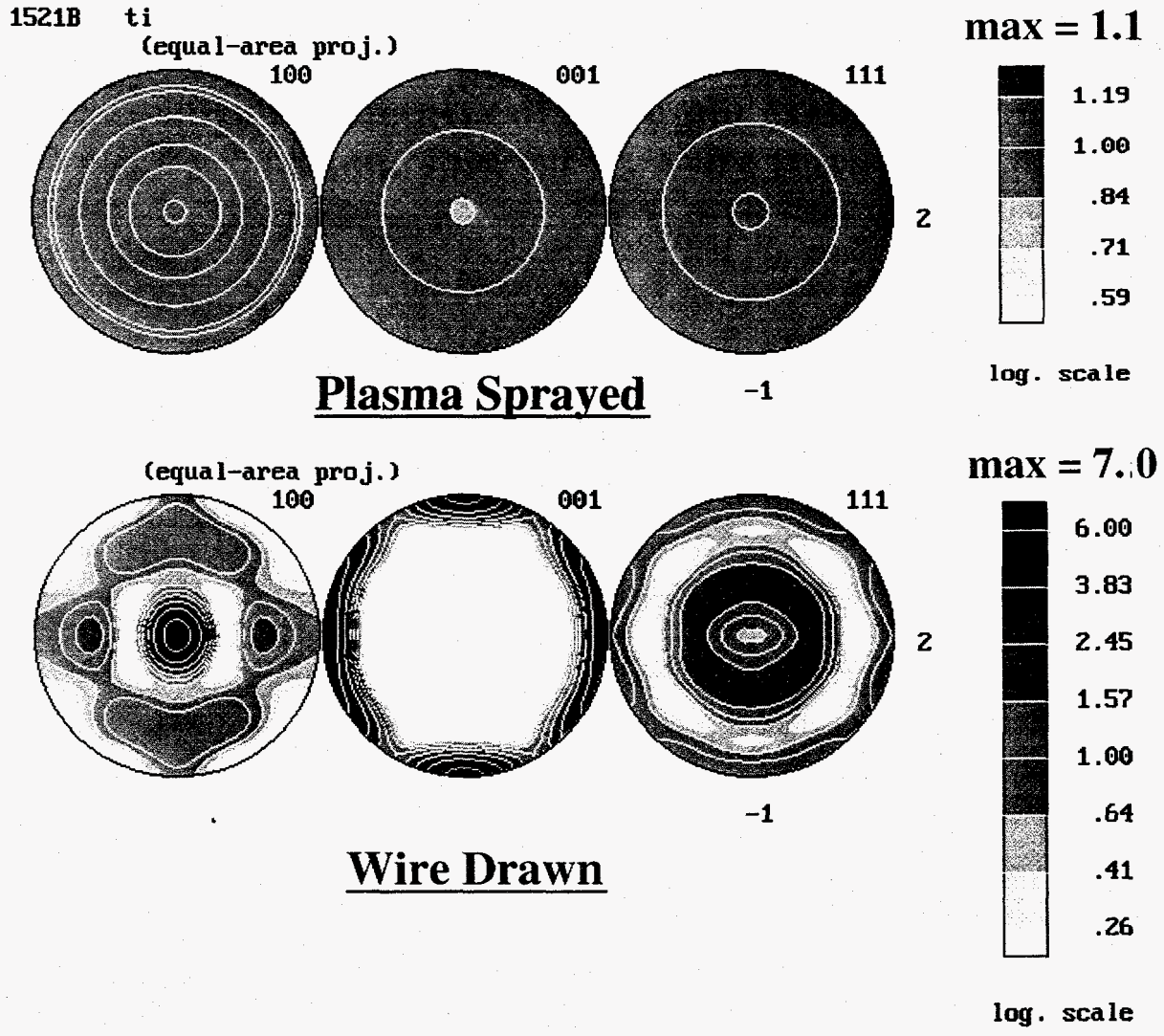

Figure 2: Pole figures for 100, 001 and 111 poles for the matrices of the PS and WD TMCs.

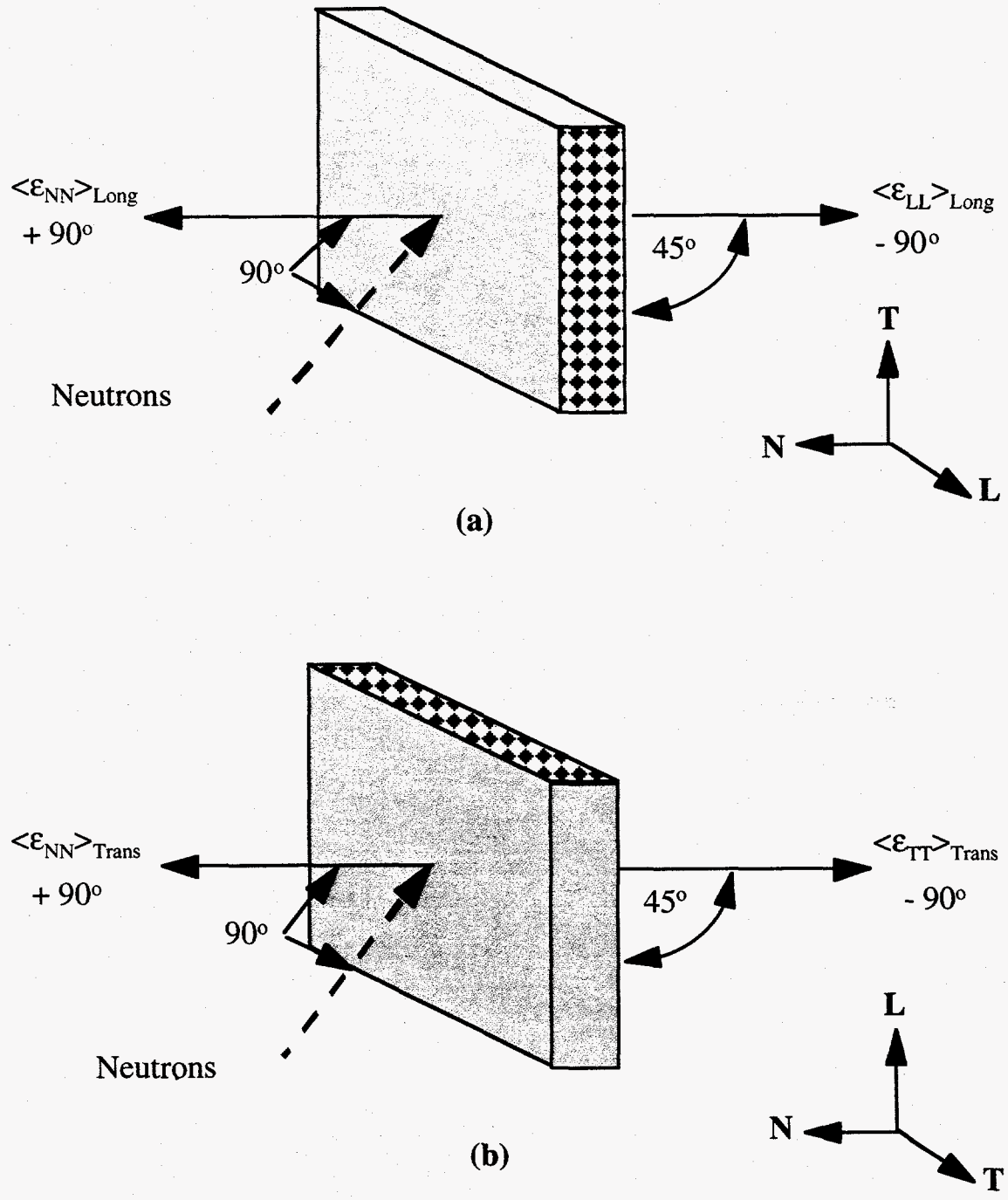

Figure 3. Schematic of the two orientations in which the samples were placed relative to the neutron beam; a) longitudinal Strain, $\langle\varepsilon_{LL}\rangle_{Long}$ and $\langle\varepsilon_{NN}\rangle_{Long}$ b) Transverse Strain measurements $\langle\varepsilon_{LL}\rangle_{Trans}$ and $\langle\varepsilon_{NN}\rangle_{Trans}$

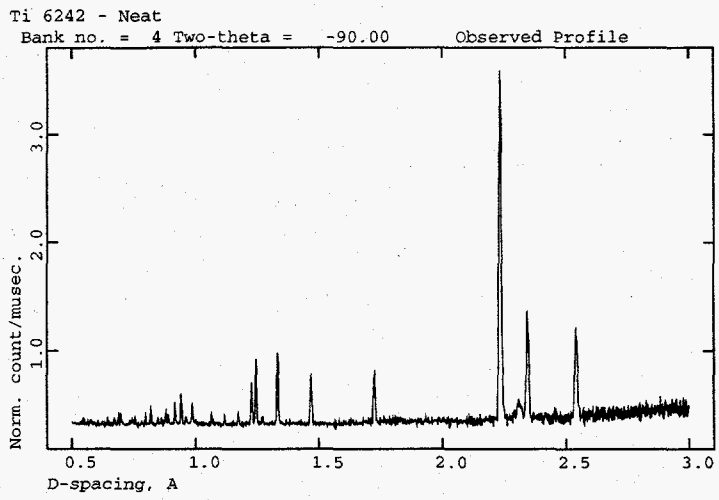

(a)

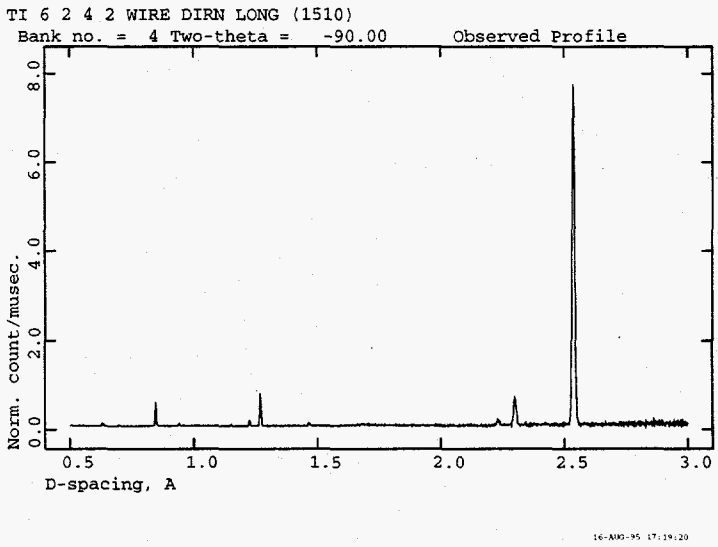

(b)

Figure 4. Diffraction plots for the monlithic Ti6242 - a) untextured b) textured matrix alloy - scattering vector in the fiber direction.

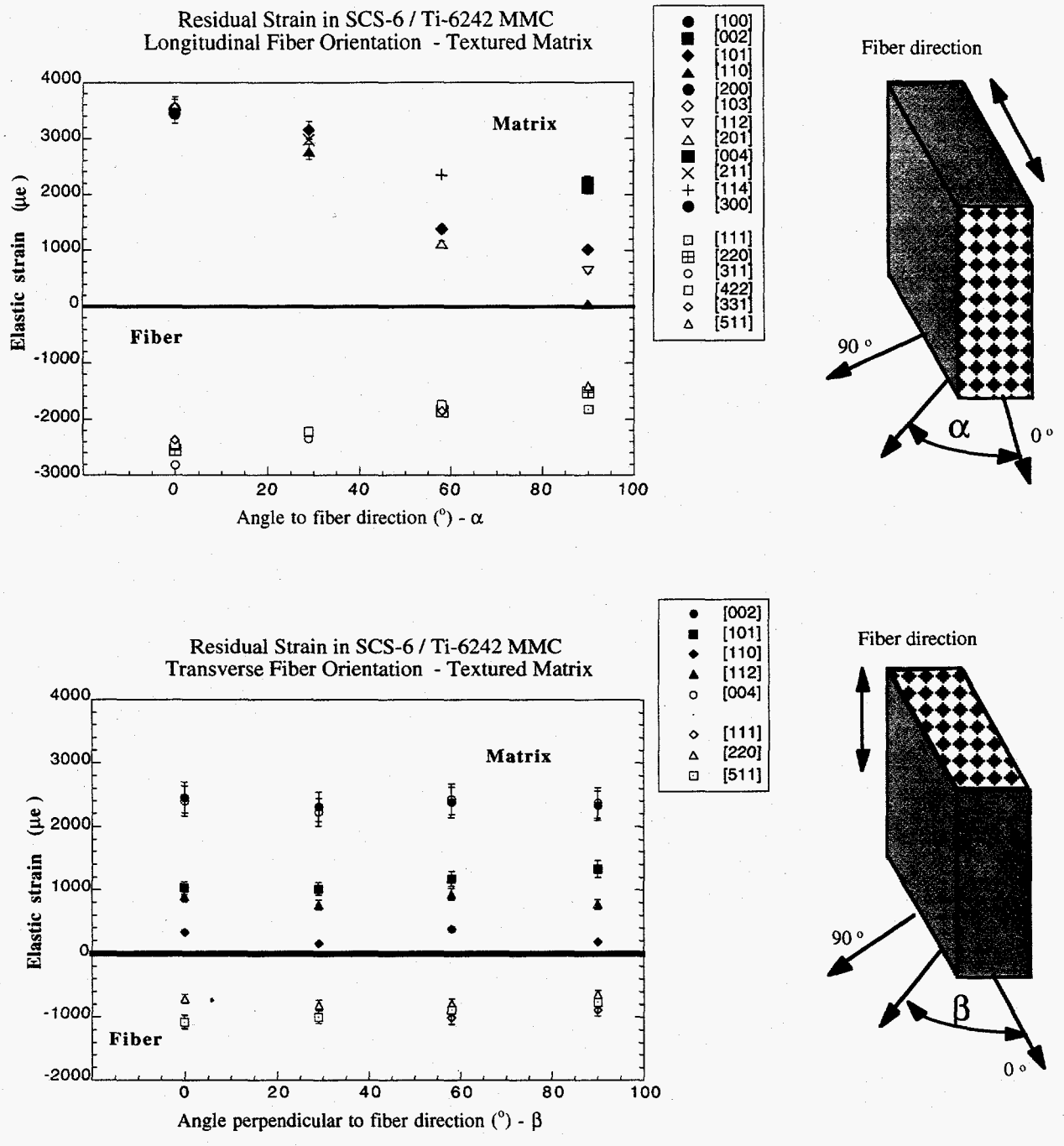

Figure 5. Neutron measured hkl strains in the textured TMC orientations as shown.

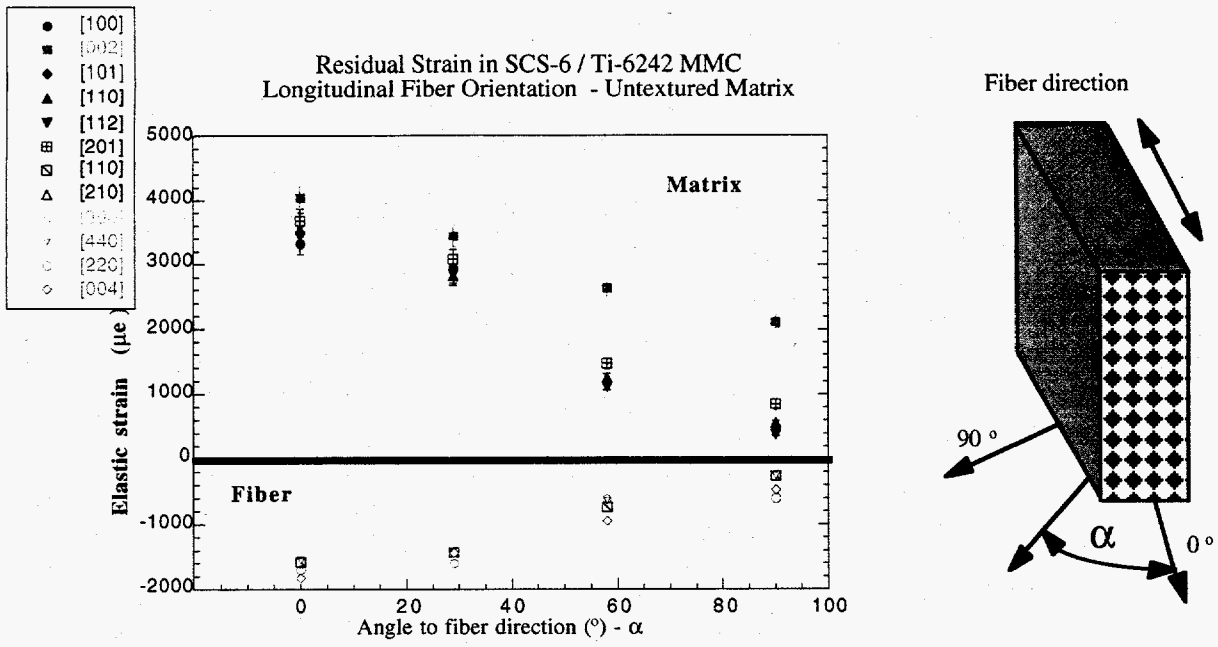

(a)

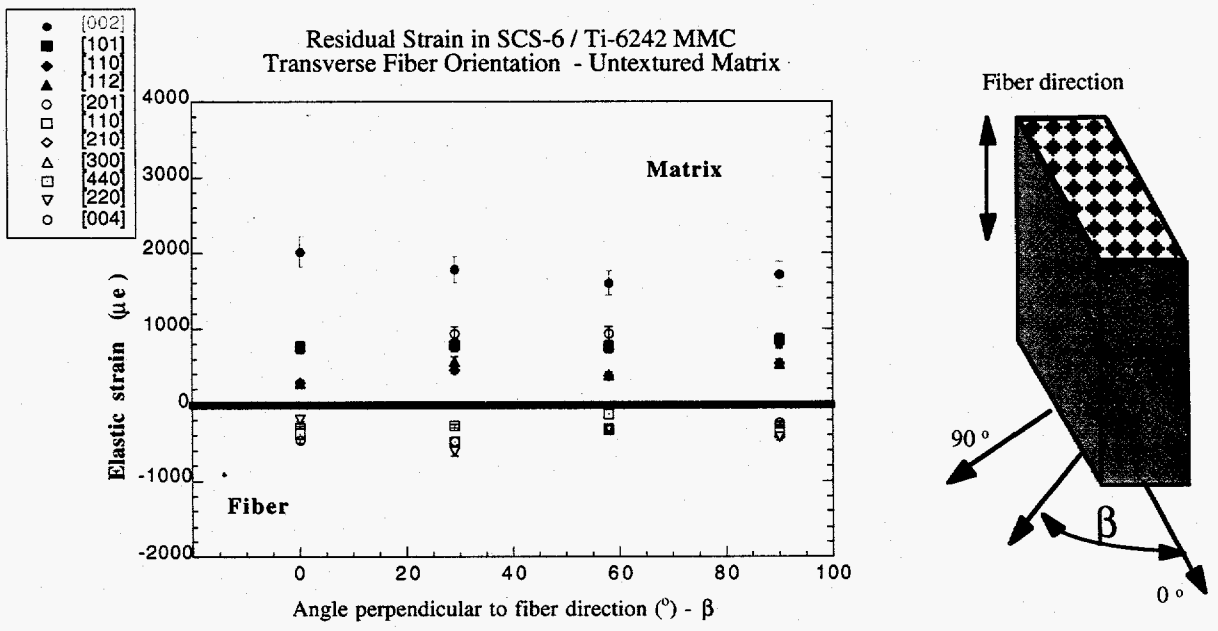

(b)

Figure 6. Neutron measured hkl strains in the untextured TMC orientations as shown

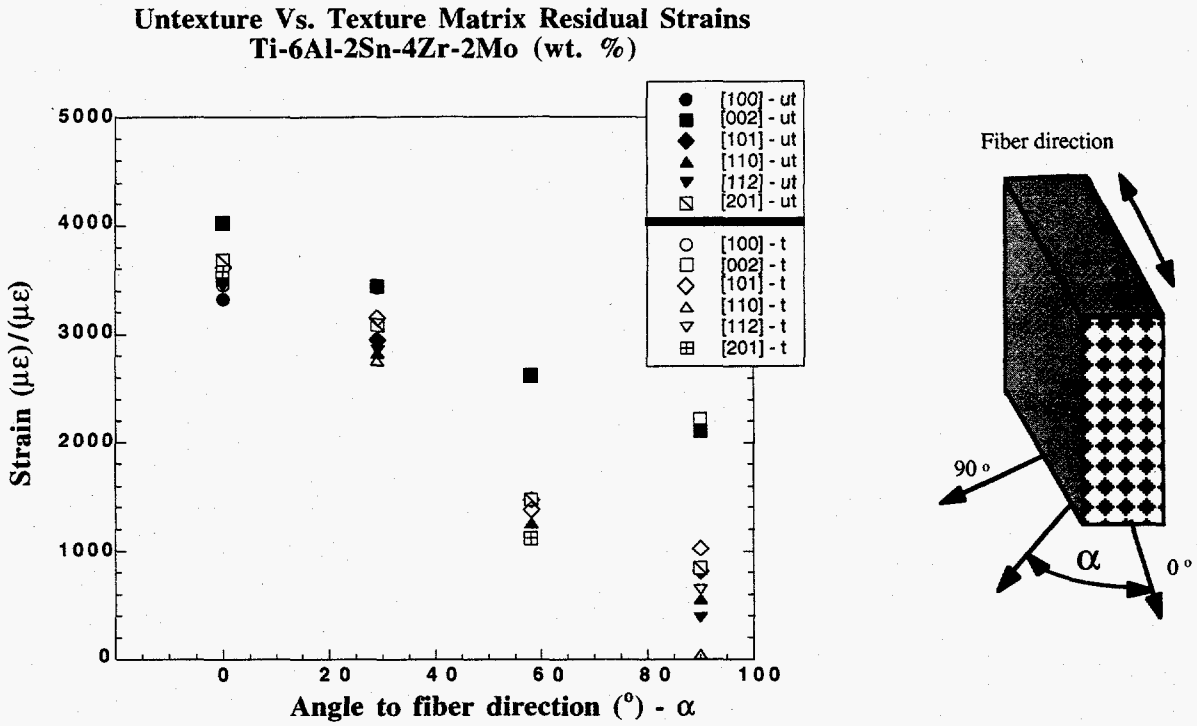

Figure 7. Comparison of the strains measured in the matrix of WD (textured) and PS (untextured) composites for the fiber orientation shown.

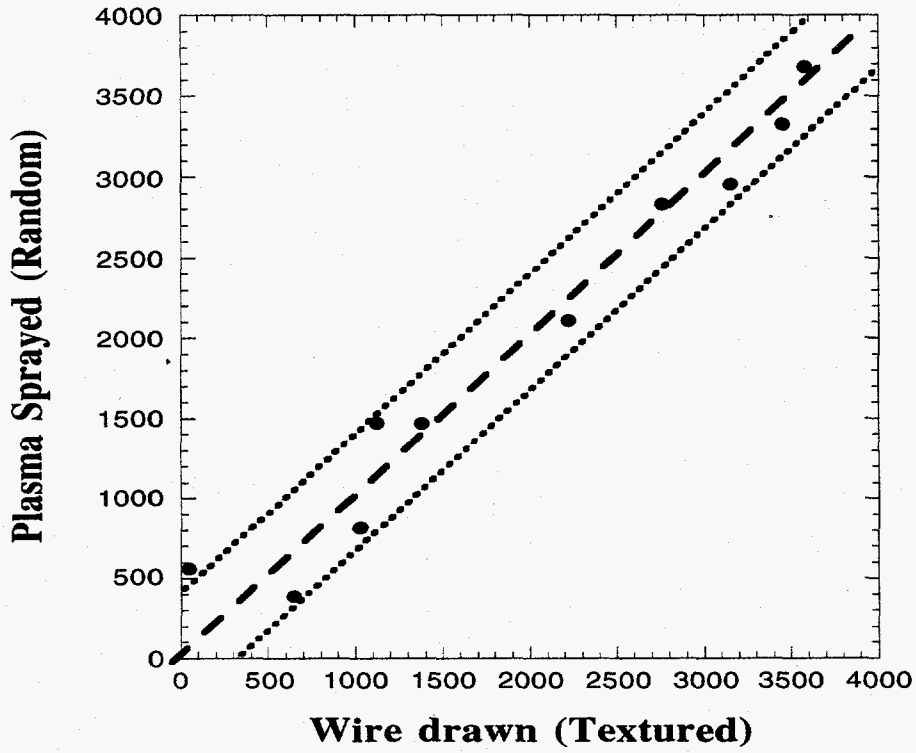

Figure 8. Comparison of the equivalent strains measured in the matrix of WD (textured) and PS (untextured) composites for the same hkls'.